Chalcogenide Letters Vol. 16, No. 6, June 2019, p. 303 - 308

SYNTHESIS, X-RAY DIFFRACTION, AND RAMAN SPECTROSCOPY OF $AgSnBiSe_3$ AND $AgSnBiSe_2S$ SYSTEMS

S. MORIS[a], P. BARAHONA[b], P. VALENCIA-GÁLVEZ[*,c], A. GALDÁMEZ[c]
[a]*Vicerrectoría de Investigación y postgrado, Universidad Católica del Maule, Avenida San Miguel 3605, Talca 3480112, Chile*
[b]*Facultad de Ciencias Básicas, Universidad Católica del Maule, Avenida San Miguel 3605, Talca 3480112, Chile*
[c]*Facultad de Ciencias, Departamento de Química, Universidad de Chile, Las Palmeras 3425, Santiago, 7800003 Chile*

$AgSnBiSe_3$ and $AgSnBiSe_2S$ were prepared by solid state reactions at 950 °C. The phases were characterized by powder X-ray diffraction (XRD), scanning electron microscopy (SEM), and Raman spectroscopy. The samples were indexed in two space groups: $Pm\bar{3}m$ (No. 221) and P4/mmm (No. 123). The Raman spectra confirmed the structure of the $AgSnBiSe_3$ and $AgSnBiSe_2S$ compounds to be distorted NaCl-type with seven characteristic signals for the Raman active modes.

(Received March 13, 2019; Accepted June 24, 2019)

Keywords: Chalcogenides, XRD patterns, Electrical characterization, Raman spectroscopy

1. Introduction

The multicomponent silver and copper chalcogenides family —$AM(1)M(2)Q_3$, where A = Ag, Cu; M(1) = Pb, Sn, Ge; M(2) = Bi, Sb, As; and Q = S, Se, and Te—contains a number of phases that are ferroelectric, thermoelectric, and dielectric [1-8]. Extensive work has been performed by Kanatzidis *et al*. to understand the properties of chalcogenide compounds, which have many promising thermoelectric attributes [2-4]. Numerous thermoelectric systems, such as $AgPb_mSbTe_{2+m}$ and $AgSn_mSbSe_{2+m}$ systems, have been developed and reviewed previously [9-11]. Experimental single-crystal X-ray diffraction (XRD) and high-resolution transmission electron microscopy (HRTEM) studies have indicated that the electrical properties of these chalcogenide compounds are related with nanoscopic inhomogeneities [3]. Recently, Kheifets *et al*. reported dielectric and ferroelectric properties in the $AMSbSe_3$ family (A = Ag, Cu; M = Pb, Sn, Ge) [1]. These phases have high relative dielectric permittivity (ε´) in the order of 1000. For example, $AgSnSbSe_3$ shows maximum values of 2540 in the transition temperature range of 100-120 K and frequency range of 0.3-1.0 kHz. Other chalcogenide compounds have been investigated because of their dielectric and ferroelectric properties, including $AgPbAsSe_3$, $CuSnSbSe_3$, $AGeAsS_3$, $(MS)_{1-x}(AAsS_2)_x$, and $(MS)_{1-x}(AgSbS_2)_x$ (A = Ag, Cu; M = Ge, Pb, or Sn) [5-8]. Impedance spectroscopy measurements at low temperatures have shown that $AgSnSbSe_3$ is a mixed (electronic-ionic) conductor and exhibits transport *via* silver cations with values of effective maximum capacitance of 1590 nF and electrical conductivity of 0.575 mS/m (at 300 K and 10 kHz) [1]. The $AMSbSe_3$ family has been synthesized by the ceramic method at high temperatures and electrical measurements have been performed with ingots of the reaction products [1, 5-7]. In this context, we targeted for synthesis and characterization of $AgSnBiSe_3$ and $AgSnBiSe_2S$ compounds. Powder XRD and Raman spectroscopy indicated that these compounds exhibit a distorted NaCl-type structure. The electrical properties of these materials were studied by the four-probe method, as described below.

* Corresponding autor: p.valencia.galvez@gmail.com

2. Experimental section

2.1. Synthesis

$AgSnBiSe_3$ and $AgSnBiSe_2S$ compounds were prepared directly by combining high-purity elemental powders (99.99%, Aldrich) in stoichiometric amounts. All manipulations were performed in an argon atmosphere. The reaction mixtures were sealed in evacuated quartz ampoules and placed in a programmable furnace. The ampoules were then heated at a rate of 150 °C/h, from 25 °C until 950 °C, and held for 16 h. Subsequently, the ampoules were cooled to room temperature for characterization.

2.2. Powder X-ray diffraction measurements

Powder XRD patterns were collected at room temperature on a Bruker D8 Advance powder diffractometer (CuKα radiation, λ = 1.54098 Å) operating at 40 kV and 25 mA, in the range of $5° < 2\theta < 80°$. The XRD patterns were indexed using CHEKCELL software.

2.3. SEM-EDS analysis

The chemical compositions of the samples were determined by scanning electron microscopy (SEM) using a Vega 3 Tescan with Bruker Quantax 400 energy dispersive X-ray spectroscopy (EDS) detectors. The analysis was performed on the compressed samples (chemical mapping).

2.4. Raman scattering measurements

Raman scattering measurements were performed using a Witec Alpha 300 System with a 532 nm wavelength excitation. The spectrometer was calibrated with a reference single-crystal Si sample (Raman peak at 520.7 cm^{-1}). The spectral data were collected at room temperature in a backscattering configuration in the spectral range of 100-800 cm^{-1}, with a laser spot of ~1 μm and laser power of 2 mW.

2.5. Electrical properties

Hall-effect measurements were performed with an Ecopia HMS-2000. The pellets for electrical measurements were uniaxially pressed at ~2.5 tons, resulting in cylindrical pellets with a 9.00 mm diameter and ~1.00 mm thickness. The Hall coefficient, ±0.552 T, was obtained from a linear fit of the Hall resistivity. Electrical conductivity was measured by the Van der Pauw method at room temperature. Gold electrical contacts were deposited on the pellets by sputtering.

3. Results and discussion

As a first step, SEM-EDS analysis was performed to determine the chemical composition of the synthesized compounds. The EDS analysis (chemical maps of several areas) together with the image of backscattering on the compressed samples revealed that the compounds were uniform with a homogeneous distribution of the elements throughout the explored region. Fig. 1 shows images of secondary and backscattered electrons of the $AgSnBiSe_2S$ compound, while Table 1 summarizes the experimental compositions of the synthesized samples.

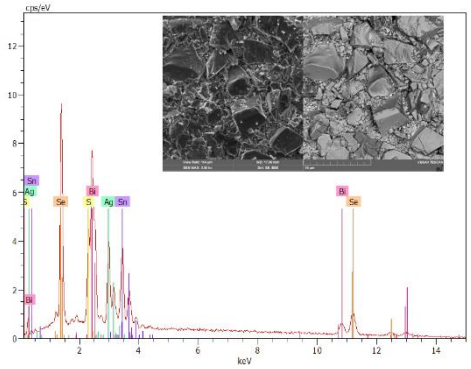

Fig. 1. SEM micrograph of $AgSnBiSe_2S$ and an example of EDS spectral analysis.

The diffraction patterns were indexed using CHEKCELL refinement routines. The $AgSnBiSe_3$ and $AgSnBiSe_2S$ compounds were successfully refined in the space group $Fm\bar{3}m$ (No. 225), and space groups of least symmetry $Pm\bar{3}m$ (No. 221) and P4/mmm (No. 123). Fig. 2 shows the indexation of the $AgSnBiSe_3$ and $AgSnBiSe_2S$ compounds in the $Pm\bar{3}m$ and P4/mmm groups, while Table 1 summarizes the cell parameters for each compound according to each space group.

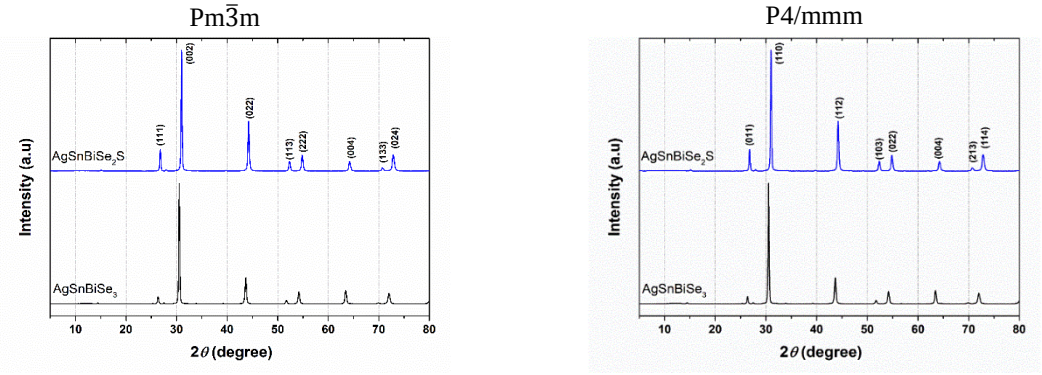

Fig. 2. Experimental powder XRD patterns for $AgSnBiSe_3$ and $AgSnBiSe_2S$.

Table 1. Lattice parameters (powder XRD data) and chemical analytical data for compounds.

Space group	$AgSnBiSe_3$			$AgSnBiSe_2S$		
	a (Å)	**c (Å)**	**Vol. (Å)**	**a (Å)**	**c (Å)**	**Vol. (Å)**
$Fm\bar{3}m$	5.8606 (19)	---	201.295	5.8142 (34)	---	196.550
$Pm\bar{3}m$	5.8606 (78)	---	201.295	5.8156 (96)	---	196.691
P4/mmm	4.1372 (20)	5.8683 (2)	100.443	4.1086 (32)	5.8402 (65)	98.583
Compositions from EDS analyses	$Ag_{1.0}Sn_{1.1}Bi_{1.1}Se_{3.2}$			$Ag_{1.1}Sn_{1.1}Bi_{1.0}Se_{2.2}S_{1.2}$		

Kanatzidis et *al.* [2], Geller et *al*. [12], Iliev *et al*. [13], and Teixeira *et al*. [14] previously published perovskite compounds (ABX_3) with rock-salt structures that presented a decrease in their symmetry. In our compounds, the cations Ag, Sn, and Bi occupy the (0, 0, 0) and (0, ½, ½) positions, while the Se (S) anion occupies (½, ½, ½) and (0, 0, ½) randomly. Therefore, the atoms in the 4a or 4b sites are no longer equivalent and indistinguishable. Moreover, the displacement of the atoms in the ideal positions and subsequent distortion of the octahedra result in a change in the symmetry of the crystal. Although these distortions are too small to be detected by powder XRD,

Raman spectroscopy—through vibration symmetry analysis—allows us to obtain the structural information.

Iliev *et al*. [13] reported a symmetry change in perovskites ($Fm\bar{3}m$) when substituted in the octahedral position by a metal B' generating a double perovskite ($Pm\bar{3}m$) and causing the distortion of the octahedrons (BX_6 and $B'X_6$) due to the change in the ion radii of the cations. In contrast, Howard *et al*. [15], proposed that double perovskites with rock-salt structure are generated if the translations (1,0,0), (0,1,0), and (0,0,1) lead to the occupation of the octahedral sites by cations B and B', while other operations of the primary space group leave the occupations unchanged. Therefore, the authors propose that in the simple perovskite $Fm\bar{3}m$, in which all the atoms are in the symmetrical center, and all phonons are forbidden by Raman [13, 15]. In comparison, the space group $Pm\bar{3}m$ presents the active A_{1g}, E_g, and F_{2g} modes in Raman [13, 15-16]. Using the method proposed by Rousseau *et al.* [16] and Krylov *et al*. [17], it is possible to obtain the distribution in terms of the irreducible representations of the point D_{4h}^{1}, corresponding to the space group P4/mmm; i.e., the active Raman modes for this group correspond to A_{1g}, B_{1g}, B_{2g}, and E_g.

Fig. 3 shows the adjustment of the Raman spectral data by Lorentzian equations of the $AgSnBiSe_3$ and $AgSnBiSe_2S$ compounds, measured under the excitation of light with a wavelength of 532 nm. It is clearly observed that the spectral profiles are similar, indicating that the compounds are arranged in the same crystal structure. Deconvolution of the experimental data allows for the identification of seven signals for the $AgSnBiSe_3$ compound, and nine signals for the $AgSnBiSe_2S$ compound. The modification of the signals at ~492 and 606 cm^{-1} for the $AgSnBiSe_2S$ phase can be attributed to the 30% substitution of sulfur at the selenium site, causing different vibrations of the network, and thus a rearrangement and doubling of the signals (to ~476 and 494 cm^{-1}, and 565 and 604 cm^{-1}). Recall that sulphur is more electronegative and its ionic radius is ~8% smaller than that of selenium. This leads to bonds with more ionic character, which give rise to new polarizations of MS_6 bonds (M = Ag, Sn, Bi) and therefore lead to changes in the strength constants.

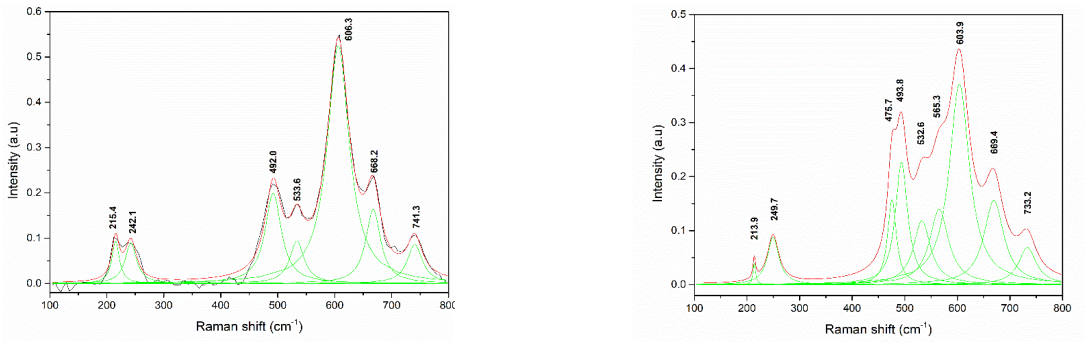

Fig. 3. Raman Spectra of the $AgSnBiSe_3$ (left) and $AgSnBiSe_2S$ (right) powder samples.

As discussed, the XRD data showed that cubic $Fm\bar{3}m$ and $Pm\bar{3}m$ and tetragonal P4/mmm space groups were possible. However, the crystallization in the $Fm\bar{3}m$ space group was discarded as it would not present active modes in Raman. On the other hand, our results show that crystallization in the space group $Pm\bar{3}m$ or P4/mmm is possible.

Electrical characterizations of the $AgSnBiSe_3$ and $AgSnBiSe_2S$ samples were performed by the Hall-effect and Van der Pauw methods [19]. The samples were *p*-type semiconductors at room temperature. The carrier concentrations were ~+10^{19} cm^{-3} in the $AgSnBiSe_3$ sample and ~+10^{18} cm^{-3} in the $AgSnBiSe_2S$ sample. The $AgSnBiSe_3$ and $AgSnBiSe_2S$ showed electrical conductivity values in the order of ~10^{0} and ~10^{-2} Ω/cm, respectively. This electrical behavior compares very well with that of other previously published analogous systems [1, 6-8].

4. Conclusions

$AgSnBiSe_3$ and $AgSnBiSe_2S$ chalcogenides were successfully synthesized by the ceramic method at high temperature from elemental powders. The purity, homogeneity, and stoichiometry were confirmed by SEM-EDS and XRD, which indicated that the samples were single phases. A chemical substitution—such as that proposed in this paper—can generate important changes in the Raman spectrum. These changes were observed when the atoms the selenium were replaced by sulfur in the same sites ((½, ½, ½) and (0, 0, ½)), generating new vibrational modes, intensity changes, and displacement of the signals, i.e., a change in the symmetry.

Raman spectroscopy provided information on the vibrational states to serve as "fingerprints," which were proportional to the crystalline quality; therefore, it can be used to monitor the replacement process in these semiconductor materials.

Acknowledgments

This work was supported by FONDECYT 1160685. We Thanks to FONDEQUIP EQM140142 for Witec Alpha 300 equipment facilities.

References

[1] O. L. Kheifets, L. Ya. Kobelev, N. V. Melnikova, L. L. Nugaeva, Tech.Phys. **52**, 86 (2007).
[2] M. G. Kanatzidis, Chem. Mater. **22**, 648 (2010).
[3] E. Quarez, K. F. Hsu, R. Pcionek, N. Frangis, E. K. Polychroniadis, M. G. Kanatzidis, J. Am. Chem. Soc. **127**, 9177 (2005).
[4] J. R. Sootsman, D. Y. Chung, M. G. Kanatzidis, Angew. Chem. Int. Ed. **48**, 8616 (2009).
[5] V. B. Zlokazov, N. V. Melnicova, E. R. Baranova, M. V. Perfiliev, L. Ya. Kobelev, Electrochim. Acta. **28**, 152 (1992).
[6] E. R. Baranova, V. L. Kobelev, O. L. Kobeleva, N. V. Melnicova, V. B. Zlokazov, L. Ya. Kobelev, M. V. Perfiliev, Solid State Ionics **124**, 255 (1999).
[7] E. R. Baranova, V. L. Kobelev, O. L. Kobeleva, L. L. Nugaeva, V. B. Zlokazov, L. Ya. Kobelev, Solid State Ionics **146**, 415 (2002).
[8] Y. F. Goring, N. V. Melnikova, E. R. Baranova, O. L. Kobeleva, Tech. Phys. Lett. **23**, 550 (1997).
[9] C. J. Vineis, A. Shakouri, A. Majundar, M. G. Kanatzidis, Adv. Mater. **22**, 3970 (2010).
[10] J. Androulakis, R. Pcionek, E. Quarez, JH. Do, H. Kong, O. Palchik, C. Uher, J. J. D'Angelo, J. Short, T. Hogan, M. G. Kanatzidis, Chem. Mater. **18**, 4719 (2006).
[11] C. B. Lioutas, N. Frangis, I. Todorov, D. Y. Chung, M. G. Kanatzidis, Chem. Mater. **22**, 5630 (2010).
[12] S. Geller, J. H. Wernick, Acta Cryst. **12**, 46 (1959).
[13] M. N. Iliev, M. V. Abrashev, A. P. Litvinchuk, V. G. Hadjiev, H. Guo, A. Gupta, Physical Review B **75**, 104118 (2007).
[14] N. G. Teixeira, A. Dias, R. L. Moreira, Journal of the European Ceramic Society **27**, 3683 (2007).
[15] C. J. Howard, B. J. Kennedy, P. M. Woodward, Acta Cryst B **59**, 463 (2003).
[16] D. L Rousseau, R. P. Bauman, S. P. S. Porto, Journal of Raman Spectroscopy **10**, 253 (1981).
[18] A. S Krylov, M. S. Molokeev, S. V. Misyul, S. N. Krylova, A. S. Oreshonkov, A. A. Ivanenko, V. A. Zykova, Y. N. Ivanov, A. A. Sukhovsky, V. N. Voronov, I. N. Safonov, A. N. Vtyurin, CrystEngComm. **18**, 8472 (2016).
[19] L. J. van den Pauw, Philips Tech. Rev. **20**, 220 (1958).